Atmospheric Pollution Research 15 (2024) 102208

Contents lists available at ScienceDirect

Atmospheric Pollution Research

journal homepage: www.elsevier.com/locate/apr

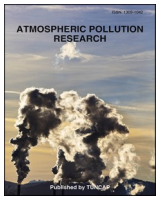

# Designing a low-cost wireless sensor network for particulate matter monitoring: Implementation, calibration, and field-test

A. Zafra-Pérez [a,*], J. Medina-García [b], C. Boente [c], J.A. Gómez-Galán [b], A. Sánchez de la Campa [a,d], J.D. de la Rosa [a,d]

[a] CIQSO-Center for Research in Sustainable Chemistry, Associate Unit CSIC-University of Huelva "Atmospheric Pollution", Campus El Carmen s/n, Huelva, 21007, Spain
[b] Department of Electronic Engineering, Computers and Automation, University of Huelva, Huelva, 21007, Spain
[c] Laboratorio de Estratigrafía Biomolecular, E.T.S.I. Minas y Energía, Universidad Politécnica de Madrid, Madrid, 28003, Spain
[d] Department of Earth Sciences, Faculty of Experimental Sciences, University of Huelva, Huelva, 21007, Spain

ARTICLE INFO

*Keywords:*
Calibration
Air pollution
Low-cost
Environmental wireless monitoring
LoRaWAN

ABSTRACT

Poor air quality can provoke severe impacts on health, necessitating environmental monitoring of atmospheric particulate matter (PM) to assess potential threats to human well-being. However, traditional continuous air quality monitoring systems are often costly and time-consuming in data treatment. Lately, there is a growing trend towards the use of low-cost wireless PM sensors, providing more detailed information than standard systems. This paper presents a system designed to measure air quality, specifically, a wireless sensor network composed of a distributed sensor network linked to a cloud system. The proposed system can efficiently measure air quality as it is cost-effective, small-sized, and consumes little power. Sensor nodes based on low-power long range (LoRa) motes transmit field measurement data to the cloud via a gateway, and a cloud computing system is implemented to store, monitor, process, and visualise the data. Advanced techniques were included in our cloud for data processing and analysis to optimise the detection of PM. Laboratory and field tests in the historic Riotinto mine validate the system's viability, offering real-time air quality information for nearby populations. Once calibrated, sensors demonstrate high accuracy, presenting mean error of −0.3% and low deviation ($R^2 = 0.96$) when compared to regulatory systems for both low (<10 $\mu gPM_{10}/m^3$) and hazardous concentrations (300 $\mu gPM_{10}/m^3$), which makes them perfect as early warning systems for atmospheric pollution in mining.

## 1. Introduction

Over the last decade, researchers have been studying air quality monitoring systems because environmental pollution in both developed and developing countries is a major health concern (Marques et al., 2019; Kim et al., 2014). Growing concern about the detrimental impact of particulate matter (PM) on human health has prompted global legislative measures. This is evident in directives like Directive 2008/50/EC from the European Parliament and Council (2008), air quality standards established by China's Ministry of Ecology and Environment China, 2016, regulations enforced by the United States Environmental Protection Agency (U. S. EPA, 2023), and guidelines provided by the European Environmental Agency (EEA, 2022). To address these concerns, the World Health Organization (WHO, 2021) has set specific concentration levels for fine PM (particles with a diameter below 2.5 μm, $PM_{2.5}$) and coarse PM (particles with a diameter below 10 μm, $PM_{10}$) to mitigate the adverse effects of air pollution. Conventional methods for monitoring air quality typically involve stationary stations equipped with various instruments or manual sampling at different locations, followed by specialized laboratory testing. Despite their general accuracy, these methods have drawbacks, necessitating the use of large, power-intensive, and expensive instruments. Additionally, skilled personnel are crucial for their proper operation, as highlighted by Idrees and Zheng (2020). Therefore, new, small, portable, scalable, and energy-efficient devices have appeared, which are less accurate than the reference instruments but yield more data points and are thus not intended to replace but to supplement them (Camprodon et al., 2019). To create cost-effective air quality monitoring systems, various types of sensors, such as electrochemical, chemoresistive, and non-dispersive infrared sensors, have been considered. These could be the building

Peer review under responsibility of Turkish National Committee for Air Pollution Research and Control.
* Corresponding author.
*E-mail address:* adrian.zafra@dfaie.uhu.es (A. Zafra-Pérez).

https://doi.org/10.1016/j.apr.2024.102208
Received 24 December 2023; Received in revised form 10 May 2024; Accepted 6 June 2024
Available online 8 June 2024

blocks for portable analysers, which would be able to communicate with either local or cloud servers and recognise alarm scenarios in the local area. However, despite the increasing accuracy of modern sensing technologies, additional validation and/or calibration are required for these devices before they can be utilised (Zafra-Pérez et al., 2023a; Dubey et al., 2022; Lung et al., 2020; Morawska et al., 2018; Fishbain et al., 2017; Clements et al., 2017).

In the field of air quality monitoring, low-cost sensors (LCS) are emerging as a promising alternative to traditional fixed-site stations. These conventional stations, known for their immobility, high expenses, and continuous maintenance requirements (Brauer et al., 2019), find a compelling counterpart in LCS. When appropriately calibrated, LCS have the ability to offer almost real-time measurements with significant spatial and temporal accuracy (Snyder et al., 2013). This capability proves valuable in identifying spatial trends in the distribution of PM in the air, as evidenced by recent studies (Giordano et al., 2021; Jovašević-Stojanović et al., 2015). The adaptability of LCS is highlighted in their recent applications for monitoring air quality in real-time. Instances include their use in vehicles for tracking city air quality (Wu et al., 2020), deployment in open-pit mines using pickup trucks and drones (Zafra-Pérez et al., 2023a and Zafra-Pérez et al., 2023b), assessment of tree damage from wildfires in forests (Price and Forehead, 2021), monitoring air quality and animal welfare on livestock farms (Tugnolo et al., 2022), and application on roads to address traffic-related concerns (Sheikh et al., 2023) and intra-urban air pollution predictions (Liang et al., 2023). This shift towards utilizing LCS not only enhances the effectiveness of air quality monitoring but also broadens its applicability across various settings and scenarios.

Current monitoring approaches in this field can be boosted using wireless sensor networks (WSNs) that make use of microcontrollers and communication technologies, enabling an adequate response in real-time and enhancing the spatial resolution of the measurements (Wang et al., 2020; Postolache et al., 2009). The selection of communication technology to be utilised in a WSN is determined by the environment and its intended applications (Yick et al., 2008; García-Martín et al., 2023). Recently, WSNs have typically used well-established devices and protocols, such as Bluetooth, Wi-Fi, and ZigBee, for applications involving short to intermediate transmission distances (Wall et al., 2021; Xia et al., 2020; Choudhury et al., 2018; Mois et al., 2017). On the other hand, applications that require minimal power consumption while operating with low data rates using long-range wireless communications, have been enabled by the emergence of low-power wide area networks (LPWANs). The LPWAN space utilises several promising technologies, such as the Narrowband Internet of Things (NB-IoT), Sigfox, and long range (LoRa) technology (Hidalgo-Fort et al., 2023; Jabbar et al., 2022; Azari et al., 2020). Among them, NB–IoT provides the highest data rate and payload size, but the fact that it operates in licenced Long-Term Evolution (LTE) frequency bands has led to its exclusion due to cost considerations. Sigfox provides a longer transmission range than LoRa, but is subject to subscription charges for each installed node, as it is deployed by network operators. Additionally, the multiple transmission of messages requires ensuring reliability, resulting in higher energy requirements. Therefore, the LoRa and LoRaWAN protocols were chosen to construct the network as a feasible option for extensively distributed measurement systems.

LoRa is a spread spectrum modulation technique based on chirp spread spectrum (CSS) technology. Its main advantage is that it operates in the unlicensed sub-GHz industrial, scientific, and medical (ISM) band. LoRa provides data rates ranging from 300 bps to a maximum of 50 kbps depending on the settings of the spreading factor (SF) and channel bandwidth (BW). The signal airtime and power consumption are determined by the transmission power (TP), SF, coding rate (CR), and preamble length (Ebi et al., 2019). LoRaWAN is a media access control (MAC) protocol developed for wide area networks with the purpose of enabling low-power devices to communicate with applications that are connected to the Internet using long-range wireless connections. LoRaWAN technology offers a range of advantageous features, including support for redundant operations, geolocation, cost-effectiveness, and low-power implementation (Lee and Ke, 2018). Devices that use LoRaWAN can be powered by energy harvesting technologies, enabling greater mobility and ease of use in the Internet of Things (IoT). Moreover, the protocol provides robust security measures such as origin authentication, integrity protection, replay protection, and full end-to-end encryption. When LoRa is used for the design of nodes and network communications, it enables the creation of low-power nodes capable of data transmission over long distances. The LoRa WAN protocol implements an authentication process between the nodes and network server as an additional step to ensure data security.

In recent years, cloud computing and the IoT have become popular emerging technologies in wireless communication (Santos et al., 2019). Cloud computing is a type of remote server that is available on the Internet and can handle requests at any time. It enables users to gain access to data or services from any device or location as long as they have access to the Internet (Arroyo et al., 2019; Botta et al., 2016; Díaz et al., 2016). Furthermore, the IoT is a network of interconnected, self-configuring devices capable of collecting and exchanging data. Cloud technology provides considerable benefits such as virtually endless storage space and significant processing power. However, limitations and disadvantages exist in these two technologies, but they can complement each other's drawbacks. In other words, the unlimited capacity, storage, and communication provided by Cloud technology can be beneficial for IoT, while the ability to interact with the "real world" is provided to the Cloud through the IoT. This type of architecture has already been implemented in various fields, such as healthcare, smart cities, and environmental monitoring (Kumar et al., 2018; Eirinaki et al., 2018; Yang et al., 2019). In addition, the combination of cloud computing and IoT has led to the development of cloud-based services that provide data storage and/or processing for IoT devices (Ray, 2016). Options for open-source projects are also available. Nevertheless, for the work presented in this paper, the decision was made to use our own cloud; accordingly, it can be customised for the specific requirements needed for our case and also to ensure independence from privately available options.

This study investigates the development of an IoT system that combines a low-cost WSN (LCWSN) with cloud services to monitor and detect air pollutants in real time inexpensively, while also providing data processing capabilities. It consists of a wireless sensing network whose sensing nodes include a data processing module (microcontroller), wireless communication module (wireless transceiver), battery, PM sensor, temperature/humidity sensor, GPS sensor, solar panel, and auxiliary elements for interfaces. The entire system is protected using a specific protection box. The network was tested and validated through its deployment in an outdoor environment. The network was put into action in a real-world scenario by deploying it at the Riotinto copper mining complex, located approximately 55 km southwest of the University of Huelva in Spain. This complex, recognized as one of the world's largest deposits of volcanogenic massive sulphide (VMS) covering an area of around 20 $km^2$, is part of the Iberian Pyrite Belt. The mining site, known for its extensive open-pit operations, releases significant amounts of PM into the atmosphere (Sánchez de la Campa et al., 2020). Since the resumption of mining activities in 2015, there has been a noteworthy release of airborne particulate matter (APM), leading to growing environmental and health concerns among the local population. The renewed mining operations have triggered apprehensions about air quality and potential health risks associated with the dust particles generated during these activities (Boente et al., 2022).

In this work, a self-sustainable wireless sensor network implements a time-unlimited autonomous operation, since the battery will always be charged during the daylight hours thanks to a small photovoltaic panel, requiring minimum human intervention. This strategy has been conciliated with low-power electronic designs at hardware level and with operation techniques in the firmware, resulting in efficient power

management. Thus, a proper choice of low power hardware components with selectable power states and a customized wireless solution with sleep periods allow achieving an optimized power consumption of the system. In addition, the WSN has been designed to fulfil other properties, such as, compact design, robustness, spatial flexibility, security, and competitive quality/price ratio, which provide a wide application prospect. Low-cost commercial off-the-shelf items were used in the hardware. An optimized method to calibrate the low-cost devices has been used to ensure the reliability of the data and make the network scientifically approved. This paper overcomes the lack of technologies for the permanent monitoring of PM in open-pit mines by detecting in real-time fugitive emissions due to daily mining operations, assessing the impact of the mine on nearby populations, and alerting remotely on unhealthy PM concentrations. Experimental results confirm the feasibility of the implementation of the wireless sensor network and the usefulness of the online monitoring of PM concentrations in air using low-cost sensors, after comprehensive calibration.

## 2. System design and implementation methodology

This section provides an in-depth description of various components of the system. It begins by outlining the architecture of the proposed WSN, followed by a description of the designed sensor nodes, which are responsible for performing measurements and transmitting data wirelessly. The network possesses a central node that receives data while also acting as a gateway, which enables a user to manage the network, server connections, and data preprocessing. A description of the entire data processing operation is also provided. Subsequently, the functioning of the gateway is explained, with the last subsection dedicated to presenting the software tools available to the end-user and the cloud system services that manage data storage and classification.

### 2.1. Network deployment

The developed system provides air quality monitoring and pollutant detection using a scalable LoRa-based sensor network in a robust and low-power configuration. The sensor network comprises two primary components, namely, the gateway and end nodes, which integrate the sensors. The readings from the sensors are stored on a local server, and a PC was used to process the data and allow visualisation. Alternatively, a front-end application can perform this process on a mobile phone. Network deployment requires the LoRa gateway to access the Internet; thus, it must be placed in a location with Wi-Fi access. Once the connection to the cloud server is established, uplink and downlink data transmissions between the server and the nodes can be carried out. In each sampling period, the nodes go through the process of performing a new measurement and sending the information, previously codified, to the server, before returning to deep sleep mode. On the server side, the data are processed and stored so that they can be later visualised using a front-end web that has been specifically developed to access and visually represent the acquired data. An illustration of the proposed system is shown in Fig. 1. To satisfy the requirements of ambient air quality measurement systems, particular considerations were applied to the design of each element of the network, regardless of the shared structure.

### 2.2. Hardware description of the sensor nodes

The sensor nodes operate as follows: Readings from the sensors are received and processed by a microcontroller, and subsequently transferred using a wireless transceiver, which is a radio frequency (RF) module that facilitates communication. Energy usage must be low; thus, the electronics of the system, from sensors and microcontrollers to conditioning interfaces and the wireless transceiver, must be low power devices. Data transmission must also be managed accordingly, as it requires significant amounts of energy.

Sensor nodes, which can collect and transmit data concerning particles present in the air, were developed to reduce cost and size. The device that enabled these measurements was an HPMA115c0-004 air quality sensor (Honeywell, 2021), which was integrated into each sensor node (Table SM1). This laser-based device can detect and count particles in the range of 0 $\mu g/m^3$ to 1.000 $\mu g/m^3$, using light scattering. The measurements were performed at the decision of the microcontroller and subsequently processed and sent via the Universal Asynchronous Receiver-Transmitter (UART) to the LoRa radio module, which transmitted them to the LoRaWAN gateway. For this application, an ATmega2560 microcontroller and RN2483 module (Microchip) were used to implement wireless data transfer at a radio frequency of 868 MHz. The data were transferred to the database can be performed at 10-min intervals. Apart from the fundamental elements of an IoT device, namely, the sensor, microcontroller, and radio module, the system also includes a number of additional elements. The MC33275DT-3.0G provides the system with a regulated 3.3 V voltage supply, which powers all the components of the system apart from the Global Positioning System (GPS) and the air quality sensor, which operate at 5 V. This additional voltage supply was obtained using a DC/DC boost converter, CE8301. Moreover, the system integrates a humidity and temperature sensor (HIH8130 from Honeywell) and an antenna, which was attached using an SMA (SubMiniature version A) connector. Finally, two IRLML9303TRPBF MOSFETs, which act as analogue switches, are used to disconnect from power supply devices that are highly energy-consuming when they are not in use. This applies to the air quality sensor and GPS, which can be deactivated (OFF state) during the time period between measurements. The switches connected both the GPS and particle sensors to the power supply and activated them (ON state) for the required duration every 10 min when new measurements were performed. This approach ensures energy efficient operation of the sensor nodes by alternating between active and low-power consumption

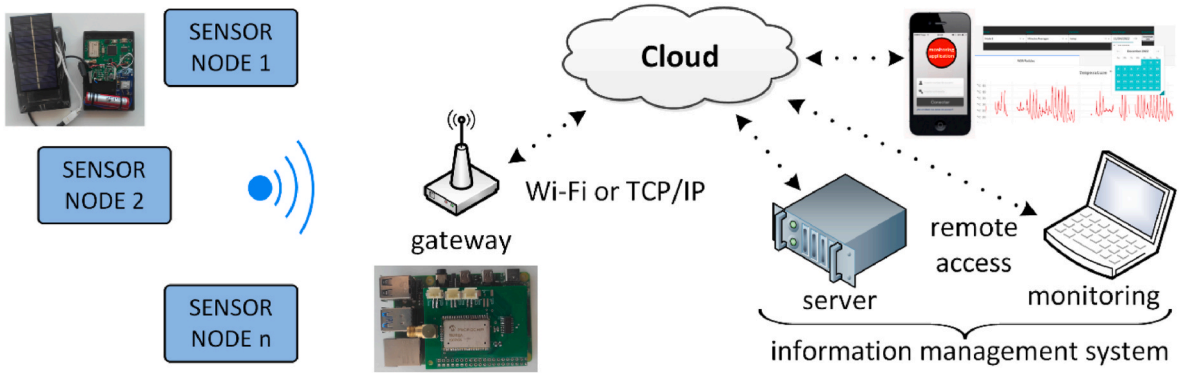


**Fig. 1.** LoRa sensor network operation scheme.

cycles.

A waterproof enclosure was used for the placement of the sensors with perforations to allow the entrance of external air and enable particle measurements. The hardware design of the network's wireless sensor nodes is shown in Fig. 2. The dimensions of the complete assembly were approximately 115 mm (L) × 70 mm (W) × 30 mm (D).

The power supply is provided by a solar panel connected to backup batteries, with the additional provision of household electricity, which is easy to access. The small 1.5 W photovoltaic panel, shown in Fig. 1, is responsible for supplying energy to the 3.7 V/3 Ah lithium battery (18650 cell) through a battery charging circuit. The average energy consumption is only 1.13 mAh due to the mentioned hardware and firmware strategies (switches and sleep mode, respectively). Thus, the sensor node is only active for a few seconds every 10 min (sampling time) taking into account the settling time of some sensors, such as, PM sensor and GPS. To reduce power consumption, the GPS has a slower sampling time than the rest of the components because in the target application the sensor nodes are located in static positions. However, for an application where the use of mobile sensor nodes is required to measure PM (Zafra-Pérez et al., 2023b), the sampling time of the GPS would need to be increased. Although the charge of the battery is maintained by the photovoltaic panel to achieve full energy autonomy, if the recharging of the system is interrupted due to unfavorable weather conditions or a failure of the photovoltaic panel, the system can be in continuous operation for 89 days without a power supply, calculated if the discharge of the battery is limited to 80% of the total.

### 2.3. Coordinator node or gateway

The developed sensor network was intended to monitor the air quality in an outdoor environment (for testing, the nodes were placed at various locations on the University Campus). A PC was used for data handling and access to a monitoring application, with access to the network provided by the coordinator node acting as a gateway for the

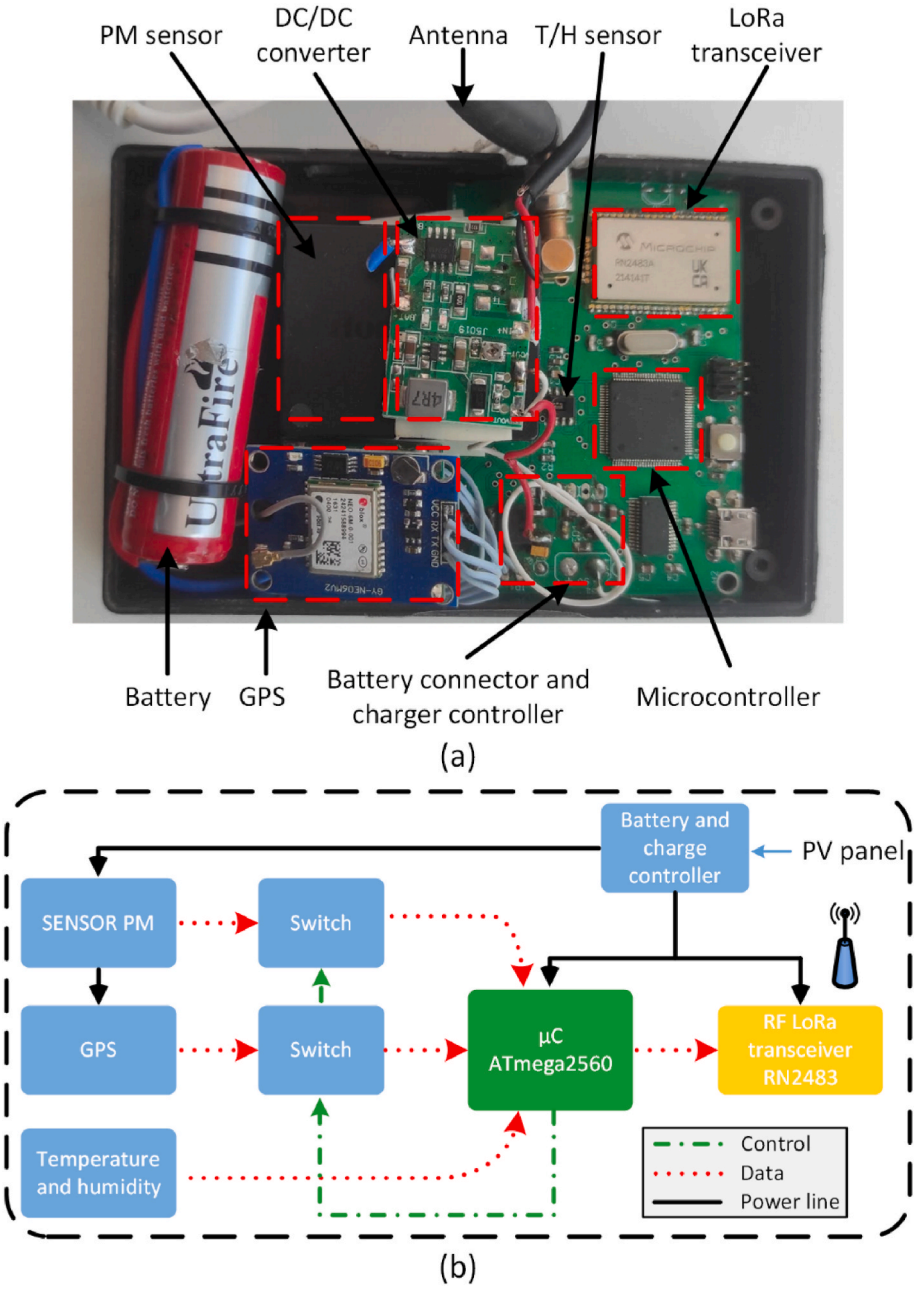


**Fig. 2.** Proposed LoRa wireless network node. (a) Hardware board. (b) Block diagram of the architecture.

system. The coordinator node includes the Microchip RN2483 wireless LoRa module and an analog to digital converter with expansion connectors to include new sensors, as shown in Fig. 3, which shows the board of the coordinator device. The data storage and functionalities that enable the visualisation of significant information regarding the entire network are provided by a Raspberry Pi, which was connected to the coordinator node via serial communication. A connection from the Raspberry Pi was also used to provide power to the coordinator node. Finally, the SMA connector enables connecting an antenna to the device.

As indicated above, a Raspberry Pi is part of the system used for data storage, calculations, and implementation of the system controller. This inexpensive computer contains a 1.4 GHz quad-core, 64-bit central processing unit (CPU), 1 GB of random access memory (RAM), and hardware providing wireless connectivity at a cost of less than $30. In addition, it provides 40 general-purpose input/output (GPIO) pins and a universal serial bus (USB) 2.0 port with a guaranteed data rate of 300 Mbps. The Raspberry Pi operating system is Linux Raspbian. The Raspberry Pi is responsible for sending data to the server and storing information in the database.

### 2.4. Programming

Fig. 4a illustrates a flowchart of the sensor nodes. After a specified time, the sensor node awakens. It activates two analogue switches (Fig. 2) and waits for a reasonable amount of time to perform all the required measurements. Thus, the microcontroller collects measurements from the PM sensor, GPS, and temperature/humidity sensors. Subsequently, the two switches are deactivated. The microcontroller sends the data to the transceiver, which transmits them to the coordinator node to be stored in the database. Proper reception is confirmed by an acknowledgement of the coordinator, and the microcontroller and transceiver enter sleep mode. After a specified time, the sensor node wakes up (and the microcontroller also wakes up to manage the sensors). In contrast, if no data are received by the coordinator, three attempts are made. If the sensor node does not receive an acknowledgement after these attempts, it performs another measurement.

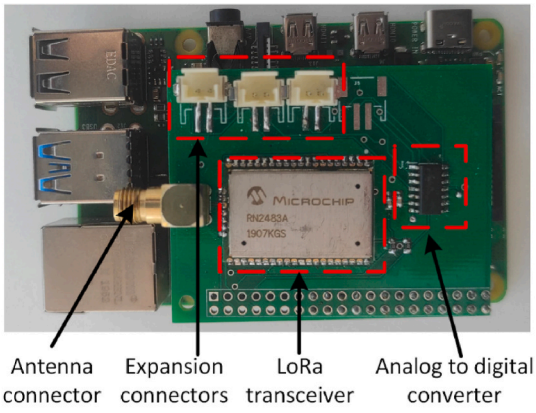


**Fig. 3.** Images depicting the coordinator node, which is connected to the Raspberry Pi (located at the bottom). (a) Top view. (b) Side view.

The programming of the coordinator node is illustrated in Fig. 4b. The program initially checks connections to the server where the data are to be saved. If there is no connection, an error is sent, and the connection is checked again. When a connection is established, concurrent programming is used, where two threads are launched from the beginning of the program. The LoRa thread reads the information that arrives from the port through which the LoRa transceiver is connected; if the data are received, it sends an acknowledgement to the sensor node. The DB thread decrypts the received information, saves it in the database, and updates the variables for monitoring.

The application running on the server was executed in Python. A flowchart of this is shown in Fig. 4c. The application begins by initialising the necessary services, and the last 100 received values are used to display the real-time monitoring information. If the Web receives any modification iteration on the dates or a change in the sensors, it updates the data through queries to the database.

### 2.5. Server database and graphical interface

The messages that arrive at the server from the nodes through the uplink must be decoded to extract data, which is performed using a payload function. Following this step, the data are formatted based on the specifications of the front-end application, that is, the graphical interface. The server implements a My Structured Query Language (MySQL) database to store the measurement data from the sensors. Consequently, the system provides a historical record of the measurements on top of the graphic interface available to the user. The front-end application was developed using Open-Source Software (OSS), which reduces overall system costs by avoiding licencing and software maintenance fees.

For data visualisation, a solution based on the Python dash library was implemented with a local server storing the data and making them available for visualisation through a Web service that can be remotely accessed through the Internet by any device. For the application to provide this remote access, the user must first provide their identification credentials, which are passed to the end-user identification service. Snapshots of the graphical interface are shown in Fig. 5. The user can select the measurements to be displayed and the corresponding date using a calendar. In addition to graphical representation, the data can also be downloaded as a Comma-Separated Value (CSV) file. Further information regarding the state of the system and its components can be consulted on different pages, with configuration options available.

The development of servers and graphical user interfaces has enabled real-time monitoring. The interface enables the user to easily visualise and access data from any sensor node.

### 2.6. Calibration of the sensor nodes and validation

The PM sensor nodes used in this study (Honeywell HPMA115c0-004) were calibrated using a reference instrument (DustTrak TSI8530) (TSI, 2024). The properties of the material and the weather conditions in our study site were not the same as those in the Riotinto mining complex. Because of this disparity, some experts stress the importance of meticulous calibration. They suggest utilizing standard equipment and recreating conditions typically encountered in real workplaces to guarantee precise sensor functionality (Giordano et al., 2021; Wallace et al., 2011).

Before starting the sampling campaign, we meticulously calibrated the PM sensor. This calibration followed the official European Commission (EC Working Group, 2010) and United States Environmental Protection Agency (U. S. EPA, 2022) protocols. Furthermore, we confirmed the accuracy of the results by validating them using regression methods, as suggested by Badura et al. (2019), including a set of

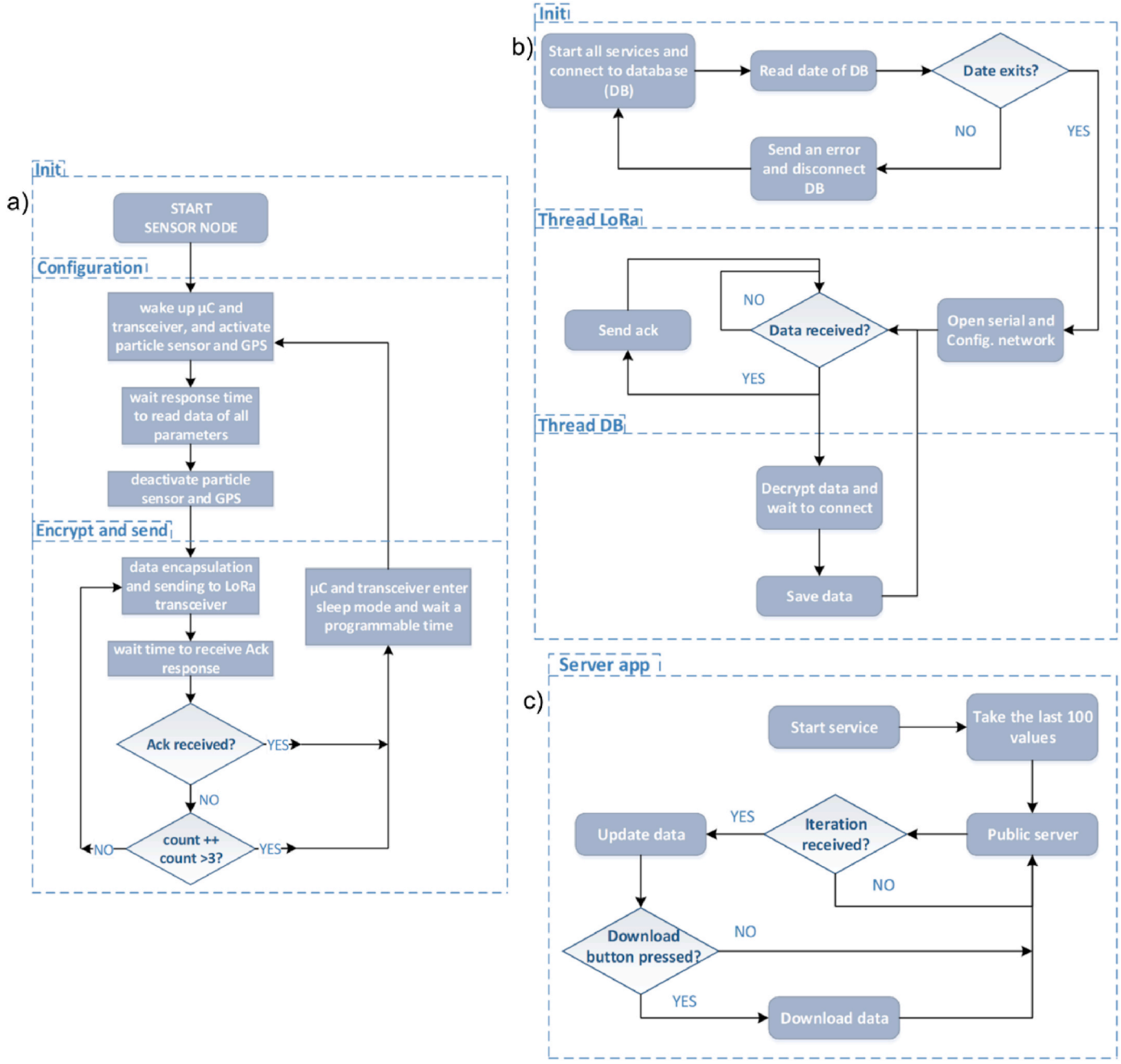


**Fig. 4.** Flow diagram for: (a) sensor nodes, (b) coordinator (gateway) node, (c) application on the server.

calibration and a set to validate results via reference devices (Beta attenuation and $PM_{10}/PM_{2.5}$ quartz fibre filters in sampling collectors, which will be described below). This calibration approach has also demonstrated its effectiveness in mining environments, as highlighted in the work of Zafra-Pérez et al. (2023), and provides insights into the sensor's performance under real conditions. Moreover, this modern methodology of calibration has been recently validated and used by other authors in similar studies (Furuta et al., 2024; Aix et al., 2023; Zimmerman, 2022).

In line with the recommendations of the United States Environmental Protection Agency, there are two approaches for evaluating low-cost PM sensors. On the one hand, we have the 'enhanced' test where the WSN is evaluated in the laboratory and on the other hand, the 'base' test, which is the one performed, where the WSN sensor is located next to regulatory grade monitors (Duvall et al., 2021; Feenstra et al., 2019; Liang and Daniels, 2022).

In pursuit of this aim, we conducted an extensive outdoor field campaign spanning 64 days, accumulating a remarkable 1549 h of continuous monitoring. In this extensive campaign, we deployed two advanced devices strategically positioned at an officially sanctioned air quality monitoring station run by the Andalusian regional government. The station, located 55 km away from Huelva city, was chosen due to its similar climate conditions. However, calibration in the nearest area was not possible due to equipment limitations. Throughout the campaign, we measured WSNs alongside two instruments. Firstly, we used a beta attenuation 5014i model (Thermo Scientific, Franklin, USA, UNE-EN 16450, 2017). This monitoring equipment at a fixed site provided continuous real-time $PM_{10}$ concentration readings with an impressive 0.1 $\mu gPM_{10}/m^3$ resolution and a time resolution of 1 s. Secondly, we employed a regulatory high-volume air sampler (MCV CAVF-PM1025, 30 $m^3h^{-1}$, Barcelona, Spain) adhering to the UNE-EN 12341 standard (2015). Equipped with $PM_{10}$ and $PM_{2.5}$ Munktell quartz fibre filters, the

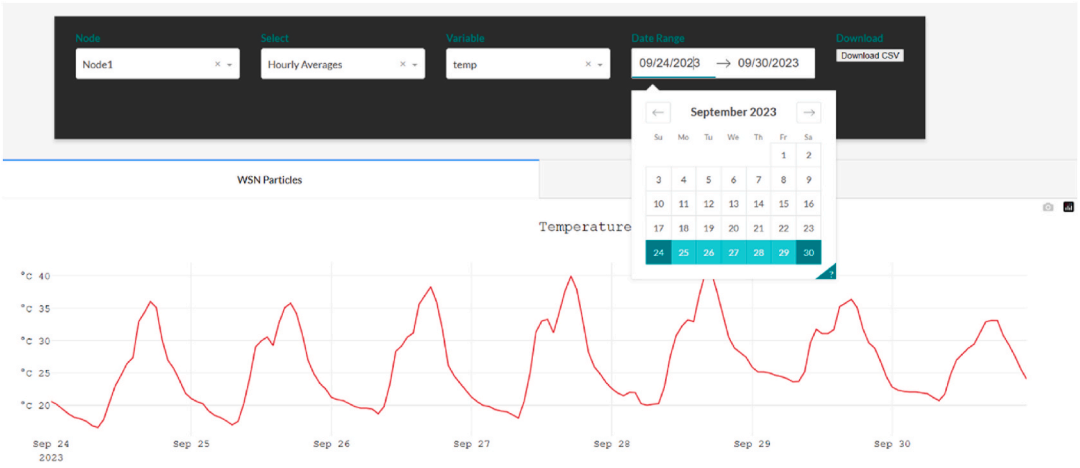


(a)

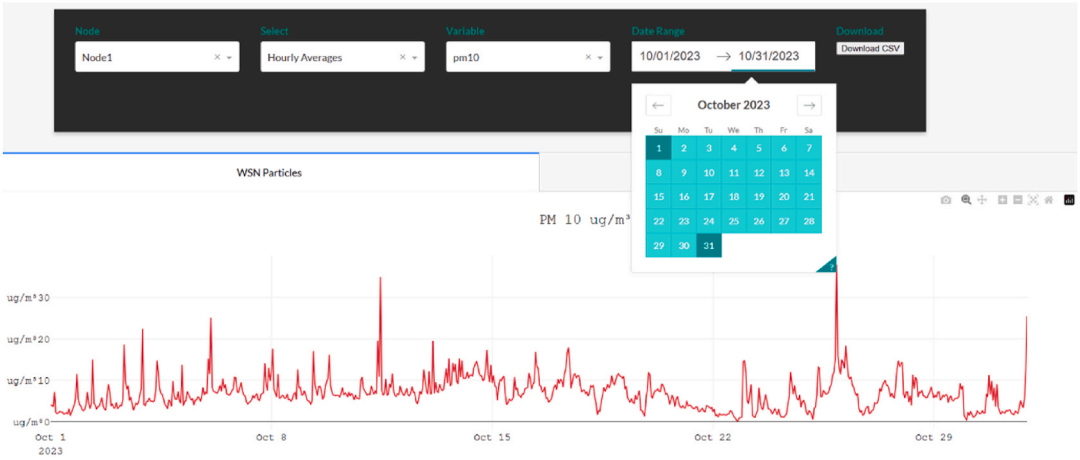


(b)

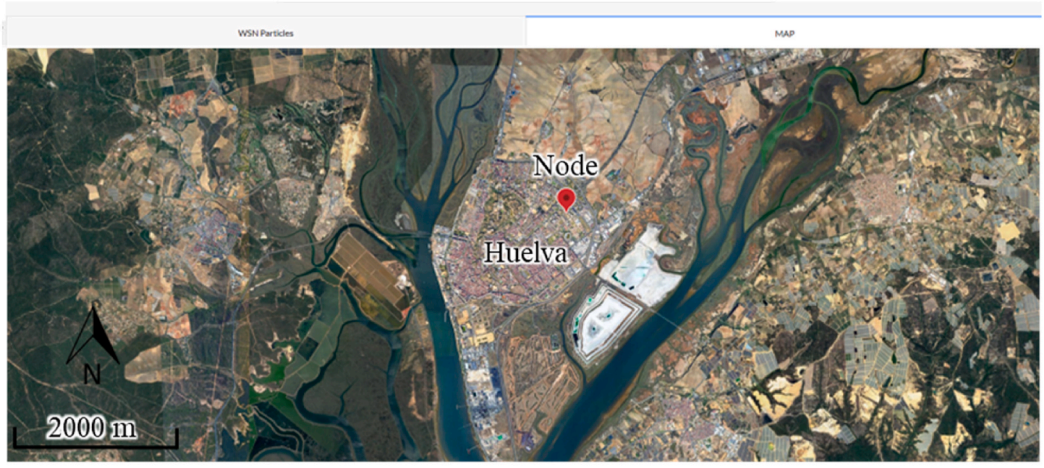


(c)

**Fig. 5.** Snapshots of the graphical user interface, where the following can be visualised: (a) temperature, (b) PM in the atmosphere, (c) location of the sensor node in the laboratory.

sampler collected PM over a 24-h period. Subsequently, $PM_{10}$ and $PM_{2.5}$ concentrations were determined in the laboratory using the gravimetric standard procedure (UNE-EN 12341, 2015). This procedure entails collecting PM from pre-weighed filters, followed by weighing after sampling and conditioning to eliminate particle-bound water, as outlined by Wallace and Hopke (2022).

To assess accuracy metrics for both hourly and 24-h averages, as recommended by Clements et al. (2022), we carefully analysed the data obtained from these instruments. The simultaneous data collection from both apparatuses provided a robust and comprehensive dataset for our

investigation.

The data treatment process for calibration closely followed the methodologies employed by prominent researchers (Zimmerman, 2022; Clements et al., 2022; Duvall et al., 2021). It underwent a transformation in time resolution during this process. The data from the WSN and beta attenuation devices, both with a shared time resolution of 1 s, could be compared directly. However, to synchronize them with the high-volume air sampler (MCV), which operates on a distinct time resolution (24 h), we needed to average all the 1-s measurements from the WSN and beta attenuation device to correspond to the 1-h and 24-h periods.

Afterward, we assessed the quality of calibration by performing linear regressions between two sets of data: 1) the measurements obtained from the WSN and the beta attenuation device, and 2) the WSN and MCV. We carefully scrutinized these linear regression analyses by comparing them with results from other researchers to ensure the robustness and accuracy of the calibration process. Once the validity of the linear regressions was confirmed, we calculated a calibration factor from the regressions involving the WSN and MCV. This calibration factor plays a vital role in refining the raw PM data directly recorded by the WSN. The corrected data aligned closely with the results obtained using the regulatory apparatus, validating the effectiveness of the calibration procedure. In addition to enhancing the reliability of the WSN measurements, the calibration process also facilitated meaningful comparisons with data collected from established and recognized monitoring instruments.

In conclusion, we employed a set of five statistical indicators to thoroughly verify the accuracy of the corrected WSN $PM_{10}$/$PM_{2.5}$ concentrations, aiming for a more reliable reflection of reality compared to the raw WSN readings (Table SM2). These indicators have shown their effectiveness in evaluating data quality for fine PM air sensors in prior research (Molina Rueda et al., 2023; Gressent et al., 2020; Wu et al., 2020). The indicators include mean bias (MB), normalized mean bias (NMB), root mean square error (RMSE), normalized mean error (NME), and normalized root mean square error (NRMSE). Detailed information about these indicators can be found in the Supplementary Materials – Part 1. To calculate these indicators, we followed the methodology outlined by Emery et al. (2017).

Here, Cr/c indicates the raw data concentration of PM measured by the WSN or the calibrated concentration of PM for the WSN, Cf denotes the concentration of PM measured by fixed-site monitoring equipment (beta attenuation or high-volume air sampler), and N indicates the number of samples.

The WSN behaviour presents a significant concern related to PM measurements, which may degrade over time owing to drift effects. While some studies, such as that of Zafra-Pérez et al. (2023), have shown that a WSN maintains long-term accuracy, others have observed potential damage that affects the measurement quality under specific external conditions (Bulot et al., 2019). Additionally, de Souza et al. (2023) discovered a notable increase in the average bias after 3.5 years. To tackle this issue, the authors recommend calibrating the sensor annually to guarantee the quality of measurements (Zafra-Pérez et al., 2023a).

## 3. Results

### 3.1. Network performance

To evaluate the communication performance between the LoRa sensor nodes and the gateway for different configurations, the nodes were positioned at various locations on a University Campus. The gateway was kept in an indoor location, the nodes were placed at different distances from the gateway, and its performance was tested for various transmission powers. The other parameters of the network configuration, that is, the carrier frequency (CF), SF, BW, preamble length, and CR, were not modified during the tests. An 868 MHz CF was used because it is one of the two licence-free radio frequency bands in the sub-gigahertz region available in Europe. A 125 kHz bandwidth was set to ensure sufficient bitrate and sensitivity to detect the radio signal. The value of the spreading factor was set to seven (maximum transfer speed), the lowest it can take, with one coding that results in the lowest time-on-air for the signal, thus reducing the energy consumption. In addition, the energy requirements were further reduced using the shortest length for the preamble. For the above configuration, the success rate of the data transfer to the server was 98%.

The sensors were placed in different buildings at a distance of just over 150 m from the gateway, with obstacles between them, that is, without a direct line of sight. This setup ensures that network performance is analysed under conditions that are not ideal for communication. During testing, the nodes were powered using a standard wall socket, yet the system design and the characteristics of the configuration were designed so that a low-power mode was used, which would enable battery-powered operation of the nodes.

### 3.2. Evaluation of WSN monitoring

Upon performing the calibration, as detailed in Section 2.6, we reveal the findings of comparing the WSN under assessment with the currently deployed devices, including the beta attenuation 5014i device and the regulatory MCV CAVF-PM1025 High-Volume Air Sampler (Fig. 6). Upon initial examination, the PM data linked to the calibrated data (illustrated in brown) demonstrate a closer match with the reference lines (depicted in purple) when compared to the raw data (shown in blue). It is evident that, by default, the WSN has a tendency to underestimate concentrations that may pose a risk, consistently reporting values below those recorded by official equipment. However, with the implementation of the new calibration method, this problem was successfully resolved, and the measurements of the calibrated LCWSN were similar to those of the reference equipment.

In this situation, calibrating $PM_{2.5}$ has shown promising results, especially when compared to similar processes in other studies that employed linear regression (Table SM3). Notably, the $R^2$ value of 0.96 for the $PM_{2.5}$ MCV CAVF-PM1025 filters is noteworthy as the second-best adjustment among calibrations for the same sensor. These outcomes are satisfactory, particularly since the equipment measures all accumulated $PM_{10}$/$PM_{2.5}$ every second across a 24-h span. It is vital to acknowledge that such variations are often linked to different weather conditions. Earlier researches by Di Antonio et al. (2018) and Malings et al. (2020) highlighted that factors such as relative humidity (RH), temperature (T), and high PM concentrations could adversely affect WSN measurements. Moreover, Magi et al. (2020) confirmed that increased RH levels can alter the refractive indices of atmospheric PM, leading to hygroscopic growth and potential measurement errors. Considering these insights, our calibration results signify significant progress in addressing potential errors related to environmental conditions, enhancing the overall reliability of the measurements.

To check how well the calibrated data matches the real measurements, we employed different statistical indicators of goodness-of-fit, alongside $R^2$. In particular, for $PM_{2.5}$, international organisations focused on air pollution; for example, the EU (EC Working Group, 2010) and the United States (U.S. EPA, 2022) have established threshold errors for these statistical indicators. A concise summary of these thresholds is provided in Table SM3, which clearly demonstrates that the calibrated WSN values successfully achieve the objectives set by the United States Environmental Protection Agency, which includes recommendations for the slope, calibration line intersection, $R^2$, RMSE, and NRMSE statistical indicators (Clements et al., 2022). All calibrated data exhibited substantial improvements compared with the raw data. Consequently, this calibration process can be confidently deemed optimal for $PM_{2.5}$, demonstrating the efficacy and accuracy of the methodology used.

Concerning the calibration of $PM_{10}$ measurements, Table SM5 offers a thorough comparison of different statistical indicators calculated using

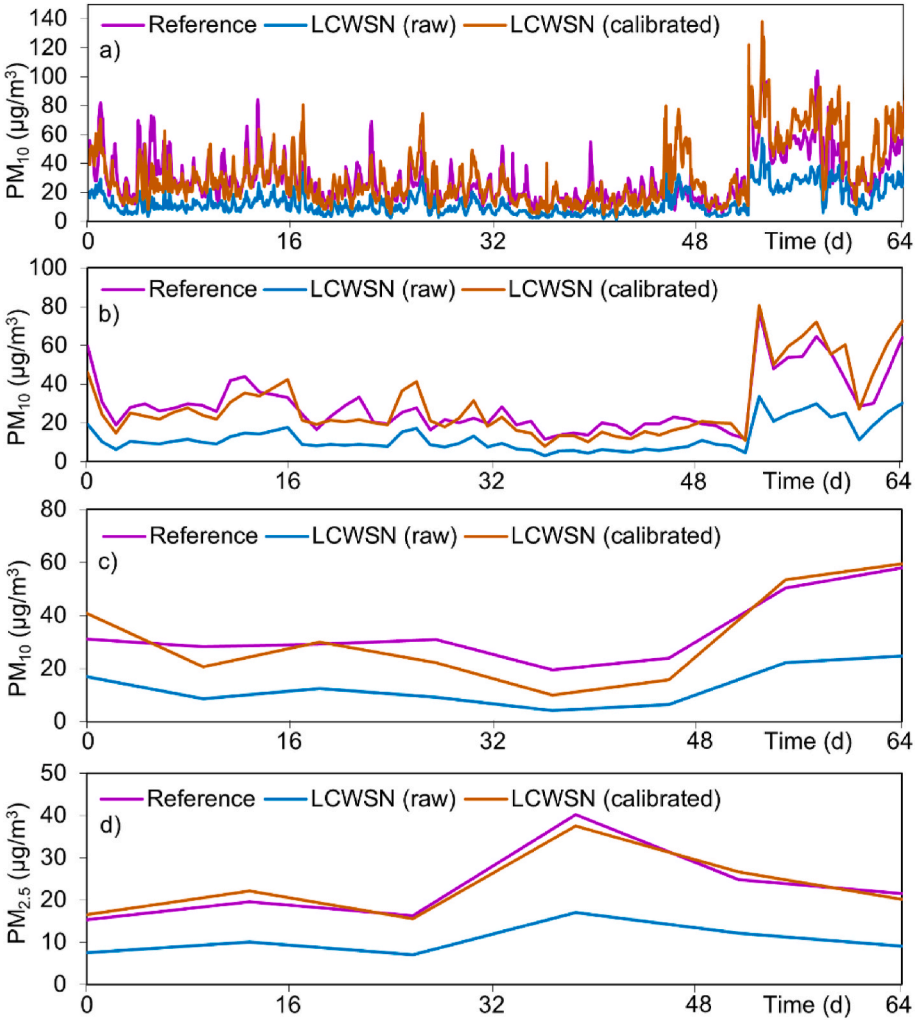


**Fig. 6.** (a) Check WSN against beta attenuation 5014i (Reference) for average 1-h $PM_{10}$ levels. (b) Compare WSN and beta attenuation 5014i (Reference) for average 24-h $PM_{10}$ levels. (c) Examine WSN versus MCV CAVF-PM1025 (Reference) for average 24-h $PM_{10}$ levels. (d) Evaluate WSN versus MCV CAVF-PM1025 (Reference) for average 24-h $PM_{2.5}$ levels.

both original and calibrated data. The calibrated $PM_{10}$ data showed a significantly closer match with the reference equipment measurements compared to the raw data. Additionally, the deviations observed in the statistical indicators were noticeably reduced for the calibrated data, indicating a substantial improvement in accuracy. Following the criteria set by Gressent et al. (2020), it is crucial to meet the condition: $|MB| \leq |NMB| \leq |RMSE| \leq |NME| \leq |NRMSE|$, ensuring accurate $PM_{10}$ concentration measurements by the sensor. In this instance, the condition is indeed met, as illustrated by the values: $|-2.33| \leq |-6.88| \leq |7.03| \leq |18.0| \leq |20.7|$. Therefore, the calibration process resulted in a significant enhancement, with the calibrated data providing measurements closely resembling those obtained using the reference equipment for $PM_{10}$. This outcome reinforces the reliability and validity of the applied calibration methodology.

According to a recent study by Hong et al. (2021), a calibrated WSN can be considered a supplementary monitor when both the NMB and NME are reduced by 20% or more. This reduction satisfies the criteria for WSN to serve various applications, including personal exposure and identification of PM (<30%), as well as education and information purposes (<50%), as stated by U. S. EPA (2014). Following calibration, the statistical indicators NMB and NME were found to be less than 20% in the calibrated WSN data, indicating that they can effectively serve as supplemental monitoring.

### 3.3. Field test in the mining environment

The WSNs were implemented in the environment of the Riotinto copper mining complex after a performance evaluation. This was performed to ensure the stability of the system, as discussed in the previous sections. The gateway is located in Cerro Colorado (an elevated location in the middle of the open-pit mining), node 1 in La Dehesa, and node 2 in Nerva, both being the closest towns to the Riotinto copper mining complex, being 1.6 km and 1.9 km, respectively from the gateway. These distances are relative to the gateway, with respect to the limit of the mining facilities these measurements are lower being from point “a" indicated on the map to La Dehesa of 0.2 km and from point “b" to Nerva of 1.4 km (Fig. 7).

In La Dehesa, the town nearest to the mine, the most concerning operations include those conducted under humid conditions, such as the dry track of the tailings pond, stockpiling, secondary crushing area, and ore loading. Nevertheless, Nerva is situated opposite the dump, an area of the mine typically characterised by minimal or sporadic activity, mainly involving the unloading of waste material by tippers (Boente et al., 2022). It is crucial to note that both towns are situated at a considerable distance from the mine and are exposed to multiple sources of pollution. For a thorough investigation into how mines affect air quality in these communities year-round, we highly suggest referring to the detailed evaluation carried out by Boente et al. (2023).

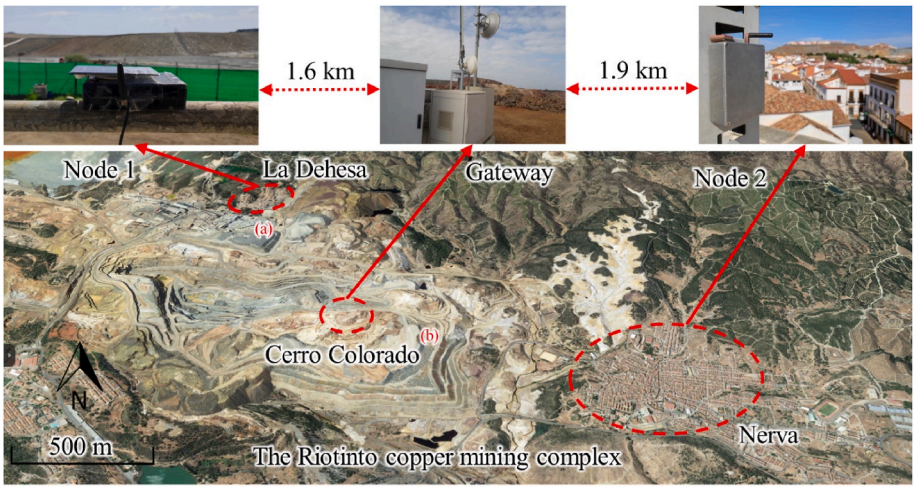


**Fig. 7.** Location of the gateway is located in Cerro Colorado, node 1 in La Dehesa, and node 2 in Nerva.

Full scalability is an important characteristic of the network; that is, the addition of nodes does not require modification of any of its parameters in the gateway. This means that the gateway can operate uninterrupted after the initial deployment, with only the newly added nodes having to be registered on the cloud server because each node must be assigned unique parameters to become part of the network. This characteristic facilitates the expansion of the network at any time with the addition of new nodes, while maintaining the overall network performance.

The escalation in PM concentrations over a specific period, precisely from February 1, 2023 to August 1, 2023 was effectively addressed. This accomplishment was enabled through the utilization of trend diagrams (Fig. 8), a level of space-time resolution that would have been unattainable in the absence of a WSN owing to the impossibility of locating wires in an environment that continuously changes, such as a mine. The visual representation in Fig. 8 vividly elucidates the intricate dispersion patterns of both $PM_{10}$ and $PM_{2.5}$ across the entire study duration, meticulously captured at node 1 and node 2 locations (Huang et al., 2019).

The observed pattern in the behaviour of the WSNs resembled that of the investigation conducted by Boente et al. (2023). In 2021, they conducted a study in identical locales of La Dehesa and Nerva, employing high-capacity regulatory air sampling equipment (MCV CAVF-PM1025, 30 $m^3h^{-1}$, Barcelona, Spain). The investigation adhered to the gravimetric standard procedure (UNE-EN 12341, 2015) for $PM_{10}$ sampling, utilizing high-purity quartz filters (Munktell®) to collect samples over a continuous 24-h period.

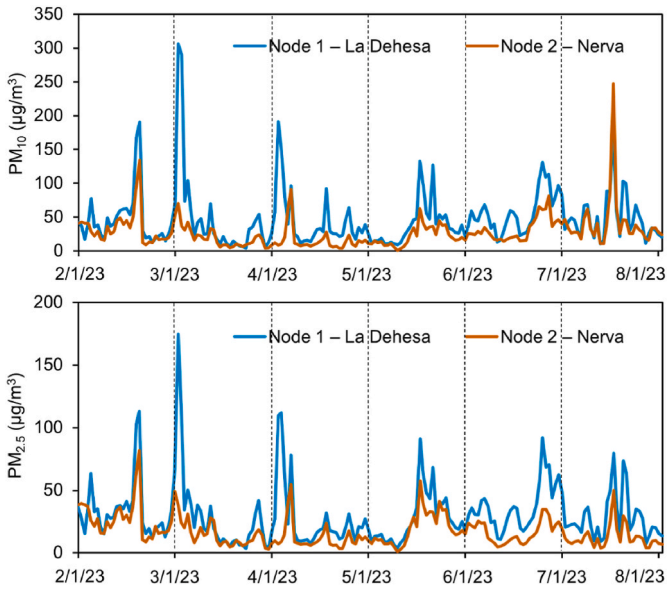


**Fig. 8.** Tendency diagram for $PM_{10}$ and $PM_{2.5}$ for the study period in node 1 and node 2.

Furthermore, the concentrations of $PM_{10}$ exhibited significant fluctuations that were influenced by the months within the timeframe. Correspondingly, the trajectory of $PM_{2.5}$ concentrations mirrored that of $PM_{10}$, albeit on a more refined scale.

Using the high level of detail that WSNs can achieve, we identified the days of the week and times of day in which PM concentrations are the highest (Fig. 9). In node 1 – La Dehesa, the hours with the highest PM concentration are from 2:00 p.m. to 3:00 p.m. because blasting occurs during that period (Atalaya Mining, 2023). In addition, they are the highest concentrations in La Dehesa because of the proximity to the mine, as shown in Section 3.3, just 0.2 km from the mining facilities and operations. In Node 2 - Nerva, the highest PM concentrations are from 8:00 a.m. to 9:00 a.m. and from 11:00 p.m. to 12:00 a.m., during which the most significant activities involved heavy road traffic, including mining trucks, as well as the town's local traffic. Conversely, in the afternoon and evening, activity subsided, as fewer individuals were at work. For week days, Node 1 has the highest PM concentrations on Mondays and Fridays, whereas Node 2 has the highest PM concentrations on Mondays and Wednesdays. On Saturdays and Sundays, PM concentrations notably decreased as fewer people engaged in work, resulting in reduced dust emissions from both mining operations and the town itself.

These findings are consistent with the characteristics of the mining complexes. This confirms the utility of the LCWSN design for monitoring PM levels. Additionally, a well-calibrated sensor enables the study of spatial and temporal trends in nearby towns. In summary, the data revealed that Node 1 (La Dehesa) exhibited higher PM concentrations than Node 2 (Nerva), primarily because of its proximity to the mining operations.

Finally, in order to assess the statistical significance between the concentration measured by the LCWSN nodes and environmental variables, a multivariate statistical regression has been performed. The aim of the analysis of multivariate regression is to use the independent variables whose values are known to predict the value of a single dependent value. Each predictor has a weight that denotes its relative contribution to the overall prediction. Multivariate regression has been used in air pollution studies with LCS to study correlation between environmental variables and LCS measures in mining ambiences

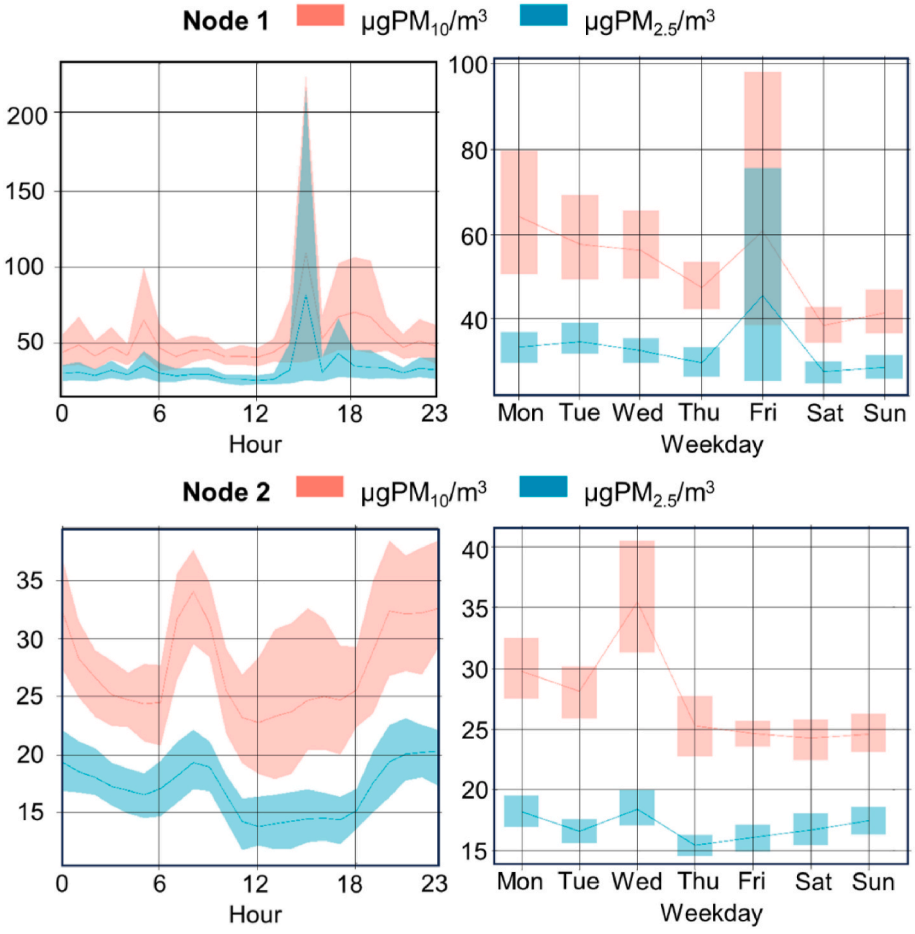


**Fig. 9.** Hourly and weekday distribution of $PM_{10}$ and $PM_{2.5}$ for the study period.

(Hongbao et al., 2024; Prasad et al., 2023). For this case, we have followed the methodology proposed by Moore et al., (2006). The dependent variable was assigned to the calibrated $PM_{10}$ and $PM_{2.5}$ measures in the two LCWSN nodes. On the other hand, relative humidity (RH), Temperature (T) and $PM_{10}$ and $PM_{2.5}$ gravimetric measures in filters were assigned the independent variables. The statistical analysis was carried out by means of the SPSS® v.24 statistical software for Windows.

The multivariate analysis yielded an R-Square value of 0.931, indicating a highly significant test adjustment. The p-values associated with LCWSN measures were 0.000 for gravimetric measures and 0.039 for temperature, both below the conventional threshold of 0.05, indicating a robust correlation consistent with prior research findings, since high temperatures trend to increase the concentrations of $PM_{10}$ and $PM_{2.5}$ in the atmosphere through resuspension. Conversely, the significance level for relative humidity (RH) was lower, at 0.117, failing to establish a statistically significant relationship between RH and the measured variables in this study. It is noteworthy that the sampling area, as reported by Boente et al. (2023), maintains consistently low humidity levels throughout the year, with a maximum RH of 63%, limiting the assessment of RH's influence on the measures. However, the Probability-Probability (P–P) plot of standardized residuals (see Fig. 10) demonstrates a linear relationship between theoretical and observed percentiles, confirming the effectiveness of the model's linearity.

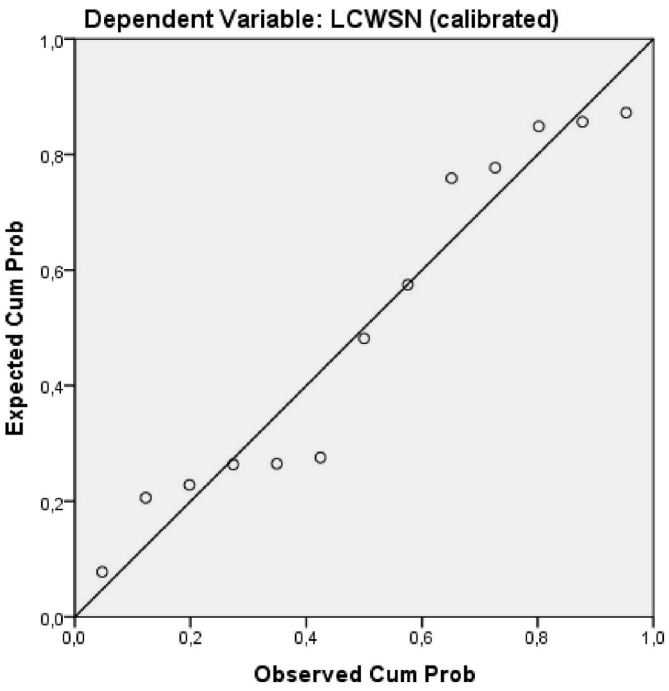


**Fig. 10.** Normal P–P plot of Regression Standarized Residual.

## 4. Discussion and future application prospect

The test and experimental results confirm the appropriate operation of the deployed WSN and the usefulness for the online measurement of PM in open-pit mines where the modern monitoring and control techniques have a very low level of use. The designed efficient

monitoring system combines low-cost sensors with a customized WSN solution based on low power techniques to achieve real-time monitoring, a self-sustainable approach, and the calibration of the devices to ensure the reliability of the data. Aspects such as data rate, synchronization, robustness against interference, security and scalability have also been considered. All this makes the sensor nodes more suitable for deployment in locations unfriendly for electronics, like the target application related to the copper extraction process in open-pit mines. Moreover, the accurate measurements due to calibrations allows for the network of low-cost sensors to be established and scientifically approved.

The custom solution presented in this work was designed to overcome some of the drawbacks of commercially available low-cost devices for outdoor air quality monitoring. The previous experience of the authors was reported in Zafra-Pérez et al., 2023a), where very tedious (and manual) tasks were necessary inside the mining facilities, transporting the sensors manually by pickup trucks for several years to detect fugitive emissions and to assess the impact of the mine on nearby populations. This methodology is hard, it requires the collaboration of the mine workers and access permissions to facilities, and the data availability is offline (and usually at an additional cost). Therefore, the designed solution based on WSN plays a key role for constant surveillance.

On the other hand, the system is referred to as low consumption according to the common concern of IoT devices for a long lifetime that is dependent on both the application and the monitored environment. Thus, the appropriate energy handling requires low power electronics for sensors, microcontroller, conditioning interfaces and transceiver. In addition, to control the sensors that waste the most energy, that is, the GPS and the PM sensor, switches have been included that deactivate them between data collection intervals. At firmware level, to reduce power consumption, the system goes into low-power standby mode between sampling intervals. The high settling time of the GPS and PM sensor to take a correct measurement sets the time that the sensor node is awake. To save energy, the GPS is only activated once a day because in this application the nodes are in static positions. Thus, the average energy consumption is 1.13 mAh, which means the system can be in continuous operation for 89 days without a power supply. Obviously, this period can be extended if the current sampling interval (10 min) is increased, or if GPS is completely disabled. Moreover, the tests of the system provided a suitable success rate of the data transfer even with obstacles between the sensor nodes and the gateway.

This work aims to have continuity by redesigning the network with a greater number of sensor nodes that can be deployed inside the mine itself to monitor in real-time fugitive emissions from daily mining operations in order to control the air quality for workers. This is a challenging task due to the difficult relations between daily mining operations, workers, mining machine traffic, and the large and aggressive work area to be instrumented. Additionally, other types of sensors can be included in each sensor node to measure other variables of interest, such as, the wind direction, which can provide information about the range of directions towards which the high concentrations of PM will travel. A more powerful microcontroller to govern the sensor nodes as well as a gateway with greater processing capacity may be advisable to support the increased data rate from the larger network. The wireless communications channel of the new LoRaWAN network must be properly dimensioned, taking into account the higher number of messages and sensor nodes. The duty cycle (DC), a crucial parameter, must not surpass 1% as per ETSI (European Telecommunications Standards Institute), which requires meticulous network design. Factors such as message sending frequency, ToA (time-on-air), SF, BW, CR, and payload must be taken into consideration. Finally, the compact design, the low power consumption, and the GPS sensor switched with a proper sampling interval also allow the sensor node to be used for mobile applications to measure PM.

All things considered, one innovative aspect lies in the utilization of LoRaWAN network connectivity, facilitating seamless live monitoring across the entire mining site. This real-time monitoring capability empowers decision-makers with actionable intelligence, enabling them to make informed choices promptly and effectively. Additionally, data collected through this network enables trend analysis and predictive modeling, further enhancing the efficacy of dust control measures over time.

Additionally, as a future prospect, the versatility of these systems extends beyond mere dust control, as they can also contribute to broader environmental management initiatives within the mining sector. For instance, by monitoring air quality parameters beyond particulate matter, such as volatile organic compounds (VOCs) or nitrogen oxides (NOx), these systems can aid in minimizing the ecological footprint of mining operations while ensuring compliance with stringent environmental regulations.

In essence, the integration of advanced monitoring and control systems represents a paradigm shift in dust management practices within open-pit mining. By embracing these sensors, specifically designed for the needs of the mining sector, enterprises can not only enhance operational efficiency and worker safety but also uphold their commitment to environmental stewardship.

## 5. Conclusions

The constant earth movement, crushing, and storage occurring in open-pit mines, especially those that are considerably large, constitute an important source of atmospheric PM. The well-known association between high PM concentrations and adverse effects on human well-being has prompted the pursuit for measures to control fugitive emissions from mines to maintain healthy environments. In this context, this study exploits wireless technologies by designing an air quality monitoring system based on unattended wireless devices that include all the components required to provide real-time monitoring of the parameters of interest. For this purpose, low-cost sensor devices with LoRaWAN communication, which guarantees reliable communication in an outdoor environment, were designed and integrated with a remote cloud server following an IoT architecture. Wireless technology provides suitable support for mining complexes, offering advantages in terms of low installation cost, scalability, lack of cabling, intelligent processing capability, high mobility, ease of deployment, and reduced maintenance. Moreover, the system is flexible because it can be adapted to different environments, and a higher number of nodes can be deployed to provide information on air quality in other areas. Testing the system confirmed the feasibility of the proposed implementation and validated the functional requirements of the developed devices and networking solution. The performance of the PM LCS was evaluated by applying correction equations based on mathematical models of linear regression and comparing them against a research-grade instrument. The system can provide mining companies with a real-time distribution of PM released during daily operations to take immediate action if unhealthy threshold levels are detected.

## CRediT authorship contribution statement

**A. Zafra-Pérez:** Data curation, Formal analysis, Investigation, Software, Visualization, Writing – original draft. **J. Medina-García:** Conceptualization, Investigation, Software, Supervision, Validation. **C. Boente:** Data curation, Formal analysis, Writing – review & editing. **J.A. Gómez-Galán:** Data curation, Investigation, Supervision, Writing – original draft. **A. Sánchez de la Campa:** Resources, Supervision, Writing – review & editing. **J.D. de la Rosa:** Conceptualization, Funding acquisition, Methodology, Project administration, Resources, Supervision, Writing – review & editing.

## Declaration of competing interest

The authors declare that they have no known competing financial

interests or personal relationships that could have appeared to influence the work reported in this paper.

## Acknowledgements

Funding for this research was provided by the project "*68/83 Contribución de fuentes del material particulado atmosférico en el entorno del distrito minero de Riotinto (2023).*" The authors express their appreciation to the Atalaya Mining Company for granting permission to conduct this research on their premises and for their wholehearted support. Funding for open access charge: Universidad de Huelva / CBUA, Spain.

## Appendix A. Supplementary data

Supplementary data to this article can be found online at https://doi.org/10.1016/j.apr.2024.102208.

## References

Aix, M.-L., Schmitz, S., Bicout, D.J., 2023. Calibration methodology of low-cost sensors for high-quality monitoring of fine particulate matter. Sci. Total Environ. 889, 164063 https://doi.org/10.1016/j.scitotenv.2023.164063.

Arroyo, P., Herrero, J., Suárez, J., Lozano, J., 2019. Wireless sensor network combined with cloud computing for air quality monitoring. Sensors 19 (3), 691. https://doi.org/10.3390/s19030691.

Atalaya Mining, 2023. Atalaya Mining plc is a European copper producer focused on providing society with the essential raw materials required for economic growth and the energy transition. https://atalayamining.com.

Azari, A., Stefanovic, C., Popovski, P., Cavdar, C., 2020. On the latency-energy performance of NB-IoT systems in providing wide-area IoT connectivity. IEEE Transactions on Green Communications and Networking 4 (1), 57–68. https://doi.org/10.1109/TGCN.2019.2948591.

Badura, M., Batog, P., Drzeniecka-Osiadacz, A., Modzel, P., 2019. Regression methods in the calibration of low-cost sensors for ambient particulate matter measurements. SN Appl. Sci. 1 (6), 622. https://doi.org/10.1007/s42452-019-0630-1.

Boente, C., Millán-Martínez, M., Sánchez de la Campa, A.M., Sánchez-Rodas, D., de la Rosa, J.D., 2022. Physicochemical assessment of atmospheric particulate matter emissions during open-pit mining operations in a massive sulphide ore exploitation. Atmos. Pollut. Res. 13 (4), 101391 https://doi.org/10.1016/j.apr.2022.101391.

Boente, C., Zafra-Pérez, A., Fernández-Caliani, J.C., Sánchez de la Campa, A., Sánchez-Rodas, D., de la Rosa, J.D., 2023. Source apportionment of potentially toxic PM10 near a vast metallic ore mine and health risk assessment for residents exposed. Atmos. Environ. 301, 119696 https://doi.org/10.1016/j.atmosenv.2023.119696.

Botta, A., de Donato, W., Persico, V., Pescapé, A., 2016. Integration of cloud computing and Internet of things: a survey. Future Generat. Comput. Syst. 56, 684–700. https://doi.org/10.1016/j.future.2015.09.021.

Brauer, M., Guttikunda, S.K., K A, N., Dey, S., Tripathi, S.N., Weagle, C., Martin, R.V., 2019. Examination of monitoring approaches for ambient air pollution: a case study for India. Atmos. Environ. 216, 116940 https://doi.org/10.1016/j.atmosenv.2019.116940.

Bulot, F.M.J., Johnston, S.J., Basford, P.J., Easton, N.H.C., Apetroaie-Cristea, M., Foster, G.L., Morris, A.K.R., Cox, S.J., Loxham, M., 2019. Long-term field comparison of multiple low-cost particulate matter sensors in an outdoor urban environment. Sci. Rep. 9 (1), 7497. https://doi.org/10.1038/s41598-019-43716-3.

Camprodon, G., González, Ó., Barberán, V., Pérez, M., Smári, V., de Heras, M.Á., Bizzotto, A., 2019. Smart Citizen Kit and Station: an open environmental monitoring system for citizen participation and scientific experimentation. HardwareX 6, e00070. https://doi.org/10.1016/j.ohx.2019.e00070.

Choudhury, N., Matam, R., Mukherjee, M., Shu, L., 2018. Beacon synchronization and duty-cycling in ieee 802.15.4 cluster-tree networks: a review. IEEE Internet Things J. 5 (3), 1765–1788. https://doi.org/10.1109/JIOT.2018.2827946.

Clements, A., Duvall, R., Greene, D., Dye, T., 2022. The Enhanced Air Sensor Guidebook. U.S. Environmental Protection Agency, Washington, DC. https://cfpub.epa.gov/si/si_public_record_report.cfm?Lab=CEMM&dirEntryId=356426.

Clements, A.L., Griswold, W.G., Rs, A., Johnston, J.E., Herting, M.M., Thorson, J., Collier-Oxandale, A., Hannigan, M., 2017. Low-cost air quality monitoring tools: from research to practice (A workshop summary). Sensors 17 (11), 2478. https://doi.org/10.3390/s17112478.

De Souza, P., Barkjohn, K., Clements, A., Lee, J., Kahn, R., Crawford, B., Kinney, P., 2023. An analysis of degradation in low-cost particulate matter sensors. Environ. Sci. J. Integr. Environ. Res.: Atmosphere 3 (3), 521–536. https://doi.org/10.1039/D2EA00142J.

Di Antonio, A., Popoola, O., Ouyang, B., Saffell, J., Jones, R., 2018. Developing a relative humidity correction for low-cost sensors measuring ambient particulate matter. Sensors 18 (9), 2790. https://doi.org/10.3390/s18092790.

Díaz, M., Martín, C., Rubio, B., 2016. State-of-the-art, challenges, and open issues in the integration of Internet of things and cloud computing. J. Netw. Comput. Appl. 67, 99–117. https://doi.org/10.1016/j.jnca.2016.01.010.

Dubey, R., Patra, A.K., Joshi, J., Blankenberg, D., Kolluru, S.S.R., Madhu, B., Raval, S., 2022. Evaluation of low-cost particulate matter sensors OPC N2 and PM Nova for aerosol monitoring. Atmos. Pollut. Res. 13 (3), 101335 https://doi.org/10.1016/j.apr.2022.101335.

Duvall, R., Clements, A., Hagler, G., Kamal, A., Kilaru, V.J., Goodman, L., Frederick, S., Jonhson Barkjon, K., VonWold, I., Greene, D., Dye, T., 2021. Performance testing protocols, metrics, and target values for fine particulate matter air sensors: use in ambient. Outdoor, Fixed Site, Non-regulatory Supplemental and Informational Monitoring Applications: Technical Report. U.S. Environmental Protection Agency, Washington, DC. https://cfpub.epa.gov/si/si_%0Apublic_record_Report.cfm?dirEntryId=350785&Lab=CEMM.

Ebi, C., Schaltegger, F., Rust, A., Blumensaat, F., 2019. Synchronous LoRa mesh network to monitor processes in underground infrastructure. IEEE Access 7, 57663–57677. https://doi.org/10.1109/ACCESS.2019.2913985.

EC Working Group, 2010. Guide to the demonstration of equivalence of ambient air monitoring methods. https://ec.europa.eu/environment/air/quality/legislation/pdf/equivalence.pdf.

EEA, 2022. Air Quality in Europe 2022. European Environment Agency, Luxembourg. https://doi.org/10.2800/488115.

Eirinaki, M., Dhar, S., Mathur, S., Kaley, A., Patel, A., Joshi, A., Shah, D., 2018. A building permit system for smart cities: a cloud-based framework. Comput. Environ. Urban Syst. 70, 175–188. https://doi.org/10.1016/j.compenvurbsys.2018.03.006.

Emery, C., Liu, Z., Russell, A.G., Odman, M.T., Yarwood, G., Kumar, N., 2017. Recommendations on statistics and benchmarks to assess photochemical model performance. J. Air Waste Manag. Assoc. 67 (5), 582–598. https://doi.org/10.1080/10962247.2016.1265027.

European Parliament and of the Council, 2008. Directive 2008/50/EC of the European Parliament and of the Council of 21 May 2008 on ambient air quality and cleaner air for Europe. http://data.europa.eu/eli/dir/2008/50/2015-09-18.

Feenstra, B., Papapostolou, V., Hasheminassab, S., Zhang, H., Boghossian, B. Der, Cocker, D., Polidori, A., 2019. Performance evaluation of twelve low-cost PM2.5 sensors at an ambient air monitoring site. Atmos. Environ. 216, 116946 https://doi.org/10.1016/j.atmosenv.2019.116946.

Fishbain, B., Lerner, U., Castell, N., Cole-Hunter, T., Popoola, O., Broday, D.M., Iñiguez, T.M., Nieuwenhuijsen, M., Jovasevic-Stojanovic, M., Topalovic, D., Jones, R.L., Galea, K.S., Etzion, Y., Kizel, F., Golumbic, Y.N., Baram-Tsabari, A., Yacobi, T., Drahler, D., Robinson, J.A., et al., 2017. An evaluation tool kit of air quality micro-sensing units. Sci. Total Environ. 575, 639–648. https://doi.org/10.1016/j.scitotenv.2016.09.061.

Furuta, D., Wilson, B., Presto, A.A., Li, J., 2024. Design and evaluation of a low-cost sensor node for near-background methane measurement. Atmos. Meas. Tech. 17 (7), 2103–2121. https://doi.org/10.5194/amt-17-2103-2024.

Giordano, M.R., Malings, C., Pandis, S.N., Presto, A.A., McNeill, V.F., Westervelt, D.M., Beekmann, M., Subramanian, R., 2021. From low-cost sensors to high-quality data: a summary of challenges and best practices for effectively calibrating low-cost particulate matter mass sensors. J. Aerosol Sci. 158, 105833 https://doi.org/10.1016/j.jaerosci.2021.105833.

Gressent, A., Malherbe, L., Colette, A., Rollin, H., Scimia, R., 2020. Data fusion for air quality mapping using low-cost sensor observations: feasibility and added-value. Environ. Int. 143, 105965 https://doi.org/10.1016/j.envint.2020.105965.

Hidalgo-Fort, E., Gómez-Galán, J.A., González-Carvajal, R., Sánchez-Cárdenas, P., Clemente-Maya, C., 2023. Battery-less industrial wireless monitoring and control system for improved operational efficiency. Sensors 23 (5), 2517. https://doi.org/10.3390/s23052517.

Honeywell, 2021. HPM series particle sensor. Advanced sensing technologies. 32322552-G-EN | G | 05/21. https://prod-edam.honeywell.com/content/dam/honeywell-edam/sps/siot/en-us/products/sensors/particulate-matter-sensors-hpm-series/documents/sps-siot-particulate-hpm-series-datasheet-32322550-ciid-165855.pdf.

Hong, G.-H., Le, T.-C., Tu, J.-W., Wang, C., Chang, S.-C., Yu, J.-Y., Lin, G.-Y., Aggarwal, S. G., Tsai, C.-J., 2021. Long-term evaluation and calibration of three types of low-cost PM2.5 sensors at different air quality monitoring stations. J. Aerosol Sci. 157, 105829 https://doi.org/10.1016/j.jaerosci.2021.105829.

Hongbao, Z., Rupeng, Z., Haibin, G., Chaonan, C., Shaoqiang, L., Shijie, J., 2024. Quantitative analysis of dust pollution characteristics and influencing factors in mining areas based on statistical modelling. J. Min. Sci. Technol. https://doi.org/10.19606/j.cnki.jmst.2024.02.011.

Huang, Z., Zhang, L., Yang, Z., Zhang, J., Gao, Y., Zhang, Y., 2019. Preparation and properties of a rock dust suppressant for a copper mine. Atmos. Pollut. Res. 10 (6), 2010–2017. https://doi.org/10.1016/j.apr.2019.09.008.

Idrees, Z., Zheng, L., 2020. Low cost air pollution monitoring systems: a review of protocols and enabling technologies. Journal of Industrial Information Integration 17, 100123. https://doi.org/10.1016/j.jii.2019.100123.

Jabbar, W.A., Subramaniam, T., Ong, A.E., Shu'Ib, M.I., Wu, W., de Oliveira, M.A., 2022. LoRaWAN-based IoT system implementation for long-range outdoor air quality monitoring. Internet of Things 19, 100540. https://doi.org/10.1016/j.iot.2022.100540.

Jovašević-Stojanović, M., Bartonova, A., Topalović, D., Lazović, I., Pokrić, B., Ristovski, Z., 2015. On the use of small and cheaper sensors and devices for indicative citizen-based monitoring of respirable particulate matter. Environ. Pollut. 206, 696–704. https://doi.org/10.1016/j.envpol.2015.08.035.

Kim, J.-Y., Chu, C.-H., Shin, S.-M., 2014. ISSAQ: an integrated sensing systems for real-time indoor air quality monitoring. IEEE Sensor. J. 14 (12), 4230–4244. https://doi.org/10.1109/JSEN.2014.2359832.

Kumar, P.M., Lokesh, S., Varatharajan, R., Chandra Babu, G., Parthasarathy, P., 2018. Cloud and IoT based disease prediction and diagnosis system for healthcare using Fuzzy neural classifier. Future Generat. Comput. Syst. 86, 527–534. https://doi.org/10.1016/j.future.2018.04.036.

Lee, H.-C., Ke, K.-H., 2018. Monitoring of large-area IoT sensors using a LoRa wireless mesh network system: design and evaluation. IEEE Trans. Instrum. Meas. 67 (9), 2177–2187. https://doi.org/10.1109/TIM.2018.2814082.

Liang, L., Daniels, J., 2022. What influences low-cost sensor data calibration? - a systematic assessment of algorithms, duration, and predictor selection. Aerosol Air Qual. Res. 22 (9), 220076 https://doi.org/10.4209/aaqr.220076.

Liang, L., Daniels, J., Bailey, C., Hu, L., Phillips, R., South, J., 2023. Integrating low-cost sensor monitoring, satellite mapping, and geospatial artificial intelligence for intra-urban air pollution predictions. Environ. Pollut. 331, 121832 https://doi.org/10.1016/j.envpol.2023.121832.

Lung, S.-C.C., Wang, W.-C.V., Wen, T.-Y.J., Liu, C.-H., Hu, S.-C., 2020. A versatile low-cost sensing device for assessing PM2.5 spatiotemporal variation and quantifying source contribution. Sci. Total Environ. 716, 137145 https://doi.org/10.1016/j.scitotenv.2020.137145.

Magi, B.I., Cupini, C., Francis, J., Green, M., Hauser, C., 2020. Evaluation of PM2.5 measured in an urban setting using a low-cost optical particle counter and a Federal Equivalent Method Beta Attenuation Monitor. Aerosol. Sci. Technol. 54 (2), 147–159. https://doi.org/10.1080/02786826.2019.1619915.

Malings, C., Tanzer, R., Hauryliuk, A., Saha, P.K., Robinson, A.L., Presto, A.A., Subramanian, R., 2020. Fine particle mass monitoring with low-cost sensors: corrections and long-term performance evaluation. Aerosol. Sci. Technol. 54 (2), 160–174. https://doi.org/10.1080/02786826.2019.1623863.

Marques, G., Pires, I.M., Miranda, N., Pitarma, R., 2019. Air quality monitoring using assistive robots for ambient assisted living and enhanced living environments through Internet of things. Electronics 8 (12), 1375. https://doi.org/10.3390/electronics8121375.

Ministry of Ecology and Environment China, 2016. Ambient air quality standards. https://english.mee.gov.cn/Resources/standards/Air_Environment/quality_standard1/201605/t20160511_337502.shtml.

Mois, G., Folea, S., Sanislav, T., 2017. Analysis of three IoT-based wireless sensors for environmental monitoring. IEEE Trans. Instrum. Meas. 66 (8), 2056–2064. https://doi.org/10.1109/TIM.2017.2677619.

Molina Rueda, E., Carter, E., L'Orange, C., Quinn, C., Volckens, J., 2023. Size-resolved field performance of low-cost sensors for particulate matter air pollution. Environ. Sci. Technol. Lett. 10 (3), 247–253. https://doi.org/10.1021/acs.estlett.3c00030.

Moore, A.W., Anderson, B., Das, K., Wong, W.-K., 2006. Combining multiple signals for biosurveillance. In: Handbook of Biosurveillance. Elsevier, pp. 235–242. https://doi.org/10.1016/B978-012369378-5/50017-X.

Morawska, L., Thai, P.K., Liu, X., Asumadu-Sakyi, A., Ayoko, G., Bartonova, A., Bedini, A., Chai, F., Christensen, B., Dunbabin, M., Gao, J., Hagler, G.S.W., Jayaratne, R., Kumar, P., Lau, A.K.H., Louie, P.K.K., Mazaheri, M., Ning, Z., Motta, N., et al., 2018. Applications of low-cost sensing technologies for air quality monitoring and exposure assessment: how far have they gone? Environ. Int. 116, 286–299. https://doi.org/10.1016/j.envint.2018.04.018.

Postolache, O.A., Pereira, J.M.D., Girao, P.M.B.S., 2009. Smart sensors network for air quality monitoring applications. IEEE Trans. Instrum. Meas. 58 (9), 3253–3262. https://doi.org/10.1109/TIM.2009.2022372.

Prasad, N., Bhattacharya, T., Lal, B., 2023. Chemometric techniques in the assessment of ambient air quality and development of air quality index of coal mining complex: a statistical approach. Int. J. Exp. Res. Rev. 36, 433–446. https://doi.org/10.52756/ijerr.2023.v36.018a.

Price, O.F., Forehead, H., 2021. Smoke patterns around prescribed fires in Australian eucalypt forests, as measured by low-cost particulate monitors. Atmosphere 12 (11), 1389. https://doi.org/10.3390/atmos12111389.

Ray, P.P., 2016. A survey of IoT cloud platforms. Future Computing and Informatics Journal 1 (1–2), 35–46. https://doi.org/10.1016/j.fcij.2017.02.001.

Sánchez de la Campa, A.M., Sánchez-Rodas, D., Márquez, G., Romero, E., de la Rosa, J. D., 2020. 2009–2017 trends of PM10 in the legendary Riotinto mining district of SW Spain. Atmos. Res. 238, 104878 https://doi.org/10.1016/j.atmosres.2020.104878.

Santos, C., Jimenez, J.A., Espinosa, F., 2019. Effect of event-based sensing on IoT node power efficiency. Case study: air quality monitoring in smart cities. IEEE Access 7, 132577–132586. https://doi.org/10.1109/ACCESS.2019.2941371.

Sheikh, H.A., Maher, B.A., Woods, A.W., Tung, P.Y., Harrison, R.J., 2023. Efficacy of green infrastructure in reducing exposure to local, traffic-related sources of airborne particulate matter (PM). Sci. Total Environ. 903, 166598 https://doi.org/10.1016/j.scitotenv.2023.166598.

Snyder, E.G., Watkins, T.H., Solomon, P.A., Thoma, E.D., Williams, R.W., Hagler, G.S.W., Shelow, D., Hindin, D.A., Kilaru, V.J., Preuss, P.W., 2013. The changing paradigm of air pollution monitoring. Environ. Sci. Technol. 47 (20), 11369–11377. https://doi.org/10.1021/es4022602.

TSI, 2024. DustTrak TSI8530. EXPMN-007. Rev. B (2/7/2024) A4. https://tsi.com/getmedia/95751f37-537d-4cbf-95e1-edc46a763764/EXPMN-007_A4_Rationale_Programming_PCF_Ambient_Monitoring?ext=.pdf.

Tugnolo, A., Beghi, R., Cocetta, G., Finzi, A., 2022. An integrated device for rapid analysis of indoor air quality in farms: the cases of milking parlors and greenhouses for baby leaf cultivation. J. Clean. Prod. 369, 133401 https://doi.org/10.1016/j.jclepro.2022.133401.

U. S. EPA, 2014. Air sensor guidebook sensor. Performance guidance. https://cfpub.epa.gov/si/si_public_file_download.cfm?p_download_id=519616.

U. S. EPA, 2022. Air monitoring methods - criteria pollutants. https://www.epa.gov/amtic/air-monitoring-methods-criteria-pollutants.

U. S. EPA, 2023. National ambient air quality standards (NAAQS) for PM. https://www.epa.gov/pm-pollution/national-ambient-air-quality-standards-naaqs-pm.

UNE-EN 12341, 2015. Ambient Air - Standard Gravimetric Measurement Method for the Determination of the PM10 or PM2,5 Mass Concentration of Suspended Particulate Matter.

UNE-EN 16450, 2017. Ambient air - automated measuring systems for the measurement of the concentration of particulate matter, PM10 (5), PM2.

Wall, D., McCullagh, P., Cleland, I., Bond, R., 2021. Development of an Internet of Things solution to monitor and analyse indoor air quality. Internet of Things 14, 100392. https://doi.org/10.1016/j.iot.2021.100392.

Wallace, L.A., Wheeler, A.J., Kearney, J., Van Ryswyk, K., You, H., Kulka, R.H., Rasmussen, P.E., Brook, J.R., Xu, X., 2011. Validation of continuous particle monitors for personal, indoor, and outdoor exposures. J. Expo. Sci. Environ. Epidemiol. 21 (1), 49–64. https://doi.org/10.1038/jes.2010.15.

Wallace, L., Hopke, P.K., 2022. Measuring particle concentrations and composition in indoor air. In: Handbook of Indoor Air Quality. Springer Nature, Singapore, pp. 517–567. https://doi.org/10.1007/978-981-16-7680-2_19.

Wang, W.-C.V., Lung, S.-C.C., Liu, C.-H., 2020. Application of machine learning for the in-field correction of a PM2.5 low-cost sensor network. Sensors 20 (17), 5002. https://doi.org/10.3390/s20175002.

WHO, 2021. WHO Global Air Quality Guidelines: Particulate Matter (PM2.5 and PM10), Ozone, Nitrogen Dioxide, Sulfur Dioxide and Carbon Monoxide. World Health Organization. https://apps.who.int/iris/handle/10665/345329.

Wu, Y., Wang, Y., Wang, L., Song, G., Gao, J., Yu, L., 2020. Application of a taxi-based mobile atmospheric monitoring system in Cangzhou, China. Transport. Res. Transport Environ. 86, 102449 https://doi.org/10.1016/j.trd.2020.102449.

Xia, K., Ni, J., Ye, Y., Xu, P., W, Y., 2020. A real-time monitoring system based on ZigBee and 4G communications for photovoltaic generation. CSEE Journal of Power and Energy Systems. https://doi.org/10.17775/CSEEJPES.2019.01610.

Yang, C.-T., Chen, S.-T., Den, W., Wang, Y.-T., Kristiani, E., 2019. Implementation of an intelligent indoor environmental monitoring and management system in cloud. Future Generat. Comput. Syst. 96, 731–749. https://doi.org/10.1016/j.future.2018.02.041.

Yick, J., Mukherjee, B., Ghosal, D., 2008. Wireless sensor network survey. Comput. Network. 52 (12), 2292–2330. https://doi.org/10.1016/j.comnet.2008.04.002.

Zafra-Pérez, A., Boente, C., de la Campa, A.S., Gómez-Galán, J.A., de la Rosa, J.D., 2023a. A novel application of mobile low-cost sensors for atmospheric particulate matter monitoring in open-pit mines. Environ. Technol. Innovat. 29, 102974 https://doi.org/10.1016/j.eti.2022.102974.

Zafra-Pérez, A., Boente, C., García-Díaz, M., Gómez-Galán, J.A., de la Campa, A.S., de la Rosa, J.D., 2023b. Aerial monitoring of atmospheric particulate matter produced by open-pit mining using low-cost airborne sensors. Sci. Total Environ. 904, 166743 https://doi.org/10.1016/j.scitotenv.2023.166743.

Zimmerman, N., 2022. Tutorial: guidelines for implementing low-cost sensor networks for aerosol monitoring. J. Aerosol Sci. 159, 105872 https://doi.org/10.1016/j.jaerosci.2021.105872.